Anomalous chaotic transients and repellers of the bouncing-ball dynamics

Marek Franaszek*
Institut für Festkörperforschung, Forschungszentrum Kernforschungsanlage Jülich G.m.b.H., D-5170 Jülich, Germany

Heikki M. Isomäki†
Faculty of Information Technology, Helsinki University of Technology, SF-02150 Espoo, Finland
(Received 27 August 1990)

An example of a strongly nonhyperbolic repeller with a continuous measure along the unstable direction is demonstrated.

It is well known that a chaotic transient is a common phenomenon in low-dimensional dynamical systems. This has been reported in many numerical as well as experimental investigations.[1] In contrast to a permanent chaotic behavior, which is connected with a chaotic attractor (defined in infinite-time limit), a chaotic transient is only observed for a long but finite time. After this the trajectory settles down on a periodic or aperiodic attractor and stays on it forever. Such behavior is associated with the existence of a nontrivial chaotic repeller.[2,3] A chaotic transient trajectory may be viewed as a walk in the close neighborhood of such a repeller. A trajectory that starts exactly from a point on a repeller would never leave it. This event has, however, zero probability. Any real trajectory starting in the vicinity of a repeller will follow it for some finite time after which it escapes from this region and never returns to it. This is nicely seen also in the present study of the bouncing-ball dynamics, where the similarity between a single long transient trajectory [Fig. 1(a)] and the numerically constructed repeller [Figs. 1(b)-1(d)] is conspicuous. A particular repeller can be viewed as an ensemble of parts of transient trajectories initiated at many different points. Thus all important quantities characteristic of a chaotic transient may be extracted from a systematic investigation of the corresponding chaotic repeller.[1]

Chaotic transients have some important characteristic features. One of them is the exponential distribution of lifetimes. Starting from different points inside the region containing a repeller one can observe trajectories with different durations distributed according to the law

$$M(n) = M_0\, e^{-n/\gamma} , \tag{1}$$

where $M(n)$ is the number of trajectories that have not escaped after n iterations and γ is a well-defined mean lifetime. Its value depends strongly on a control parameter λ of the system

$$\gamma(\lambda) \sim (\lambda - \lambda_c)^{-\sigma} , \tag{2}$$

where λ_c is the critical control for which the boundary crisis[4] takes place and σ is the divergence exponent. Another characteristic feature of a repeller related to a chaotic transient is its double-cantor structure. Typical attractors can be viewed as a product of a continuum and a fractal set with a smooth measure in the unstable direction. Contrary to this the measure on a chaotic repeller has discontinuities and characteristic holes transversal to the unstable direction. It is also a common belief that typical repellers are hyperbolic since the vicinities of tangencies should be mapped out of the region of interest. Thus if all nonhyperbolic points were mapped out then the study of the remnant structure would be easier and many difficulties which are present for typical, i.e., nonhyperbolic, attractors[5] can be safely avoided. In this paper we demonstrate that these typical features need not be rigorously true in every case and therefore a chaotic transient may in fact be a more complicated phenomenon.

The system that exhibits such unusual behavior is the well-known bouncing-ball model, which can be viewed as an extension of the dissipative Zaslavsky map.[6-8] In the model a ball is jumping in a constant gravitational field on a sinusoidally vibrating surface $v_s(\theta) = \lambda \sin\theta/(1+k)$. The moment of collision $\theta_i (\mathrm{mod}\ 2\pi)$ and the velocity v_i, with which the ball starts to fly just after the ith impact, can be obtained by iterating the dimensionless map

$$v_{i+1} = k(2\tau_i - v_i) + \lambda \sin\theta_{i+1} , \quad \theta_{i+1} = \theta_i + \tau_i \tag{3}$$

where τ_i denotes the time interval between two successive impacts satisfying the equation

$$-\tau_i^2 + v_i\tau_i - \frac{\lambda}{1+k}\cos\theta_i = -\frac{\lambda}{1+k}\cos(\theta_i + \tau_i) . \tag{4}$$

Thus starting from a given (v_i, θ_i) we can solve numerically Eq. (4) and find τ_i. When substituted into Eq. (3) the new point (v_{i+1}, θ_{i+1}) is determined and the whole procedure can be repeated. A nice feature of the dynamics is that they are demonstrable via mechanical experiments, which makes quite accurate tests possible.[9-15]

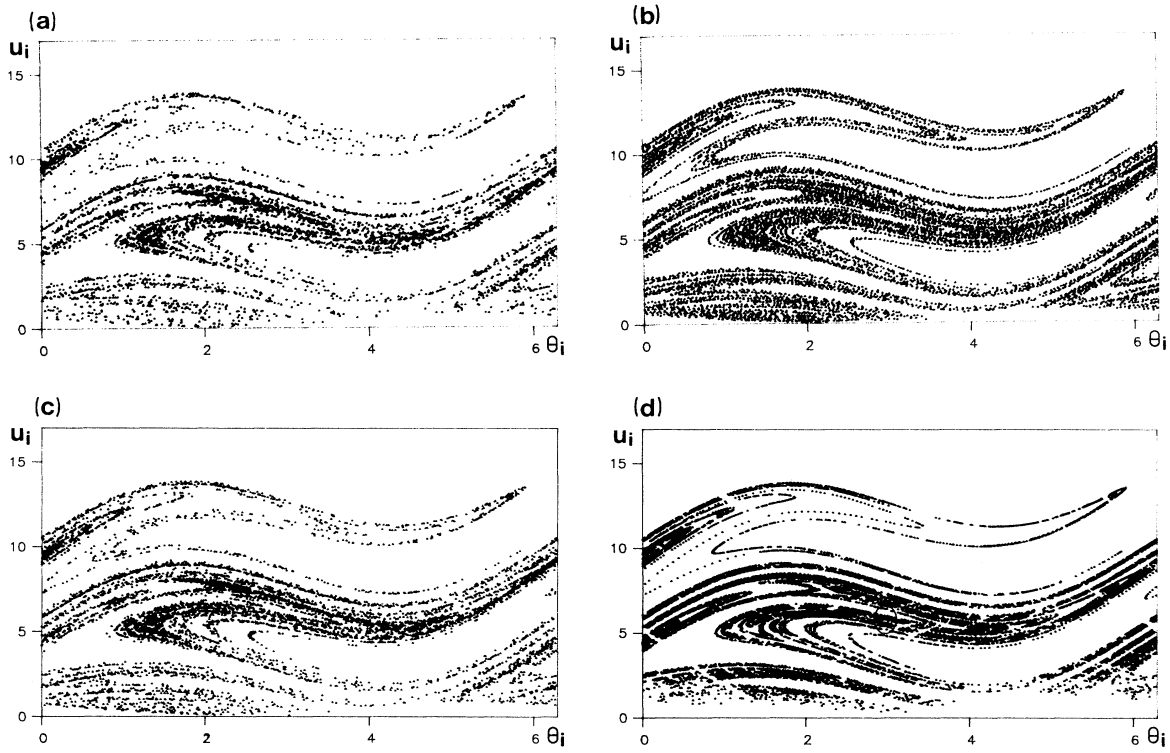

FIG. 1. Phase figures (u_i, θ_i) for $\lambda = 4.95$ and $k = 0.86$, u_i is the relative velocity. (a) Single trajectory of length 5000; (b) repeller obtained by means of the ensemble method with $n_1 = 200$, $n_2 = 1100$, and number of different trajectories $n_0 = 500$ (we plot only trajectories reaching $\tau_i < \delta$); (c) trajectory of length 3200 generated by PIM so that it stays within a small distance $\epsilon = 0.002$ from the repeller; (d) overlap of stable and unstable manifolds of the unstable fixed point (u^*, θ^*), the position of which is marked by a small ellipse, the ploted points are centers of small boxes (width 0.01 and height 0.02) inside of each we can find at least one point from the stable and one from the unstable manifolds, here $m_s = 10^5$ and other parameters as in Fig. 3. Note the similarity between (a)–(d) and Fig. 3(a).

The model has two parameters: λ, which is proportional to the amplitude of surface vibration, and k, which stands for the coefficient of restitution (all variables and parameters are rescaled to the dimensionless form). Our system is dissipative due to nonelastic impacts with $k < 1$. In experimental study the latter one was kept constant ($k = 0.86$) and amplitude λ was changed as a control parameter.[9]

For a given λ the dynamics usually exhibit multiple attractors. Hence when an initial condition from a given basin of attraction is iterated forward it will asymptote a particular coexisting attractor.[16] However, besides the permanent stationary motion there also exist regions in the (v, θ) plane where the self-reanimating transient chaos takes place.[15] During this motion the ball may temporarily stick to the surface when $\tau_i \approx 0$ and $\theta_i \notin [\theta_1^*, \theta_2^*]$, where

$$\frac{\lambda}{1+k} \cos\theta_{1,2}^* = -2 \ . \tag{5}$$

The subinterval $[\theta_1^*, \theta_2^*]$ is the set of initial phases from which the peculiar self-reanimating chaos can be initiated with a zero relative velocity for a suitable $\lambda > 2(1+k)$ (in the continuous motion the detachment occurs at the first possible moment θ_1^*). Although this is an important part of the bouncing-ball dynamics we exclude this phenomenon from the current consideration for the sake of clarity. If $\tau_i \approx 0$ we can expand the right-hand side of Eq. (4) up to the quadratic term [linear approximation gives the trivial result $v_i \approx v_s(\theta_i)$] and we obtain

$$\tau_i \approx \frac{u_i}{1 + [\lambda/2(1+k)] \cos\theta_i} \ , \tag{6}$$

provided that θ_i is not too close to θ_1^* (if it is, then higher terms are needed but still θ_i must be kept out of the interval $[\theta_1^*, \theta_2^*]$). Inserting Eq. (6) into (3) we get

$$u_{i+1} \approx k u_i \ , \tag{7}$$

where the relative velocity of the ball with respect to the vibrating surface is $u_i = v_i - [\lambda/(1+k)] \sin\theta_i$. Equations (6) and (7) mean that whenever the trajectory visits the neighborhood of such a point (v_i, θ_i) for which $\tau_i \approx 0$,

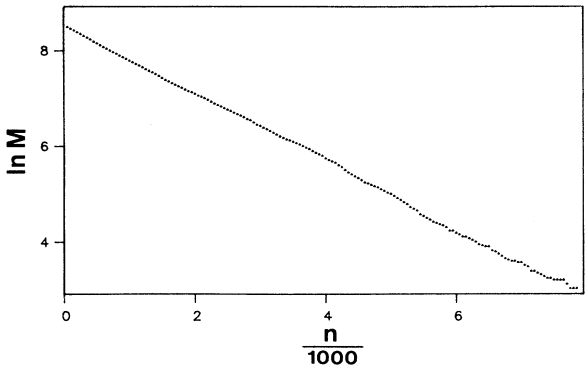

FIG. 2. Distribution of life times $\ln M(n)$ vs number of iterations n for $\lambda = 4.95$. Number of initial points $M_0 = 600$ [Eq. (1)].

we observe a sequence of points (v_j, τ_j) monotonically converging to the limit $(v_s(\theta), 0)$, where $\theta = \theta_i + \sum_{j=1}^{\infty} \tau_{i+j}$. The limit point $(v_s(\theta), 0)$ has a simple physical meaning. Namely, the jumping slows down and the ball finally stops on the vibrating surface in contact with it until the phase θ_1^* is again reached. This standstill is the system's natural ground-state attractor, which is observed both in computations as well as in experiments.[15,16] In practical computation the sticking to the surface takes place when τ_i reaches some small, finite number δ.

Before the system starts to approach its ground state it may evolve over a long time in a complicated way. Figure 1(a) gives an example of a single trajectory. Iterations of the map (3) and (4) are ended when τ_i becomes less than $\delta = 0.01$. Starting from another initial point we can observe a trajectory which usually has a very different duration. In order to determine the distribution of lifetimes we take a large number of different initial points uniformly distributed on the (u, θ) plane and iterate each of them as long as $\tau_i > \delta$. As can be seen in Fig. 2 the resulting distribution satisfies the exponential law of Eq. (1) very well, with the mean lifetime $\gamma \approx 1350$. This value of γ is relatively large, but excellent agreement with Eq. (1) may suggest that we are dealing with a typical chaotic transient. Therefore at the next step we try to find a chaotic repeller which could be responsible for the existence of this transient. However, we find a repeller which certainly does not look typical. In order to be sure that its anomalous properties are not caused by any particular numerical method used in generating the repeller, we construct it by three different independent procedures: by the ensemble method,[3] by the proper interior maximum method with three line-segment points (the PIM triple procedure),[17] and by the method[1] of overlapping stable and unstable manifolds of a saddle.

In the ensemble method[3] we plot many trajectories resulting from forward iterations (as long as $\tau_i > \delta$) of a large number of initial points but from each single trajectory we discard the first n_1 as well the last n_2 iterations; see Fig. 1(b). In spite of the fact that $n_2 \sim \gamma$, we have not found any holes transversal to the unstable direction that are supposed to be characteristic of chaotic repellers.

A similar result is obtained when we apply the PIM triple method.[17] This procedure was successfully used to construct repellers in many systems. Strictly speaking this procedure allows one to generate an arbitrarily long trajectory which stays arbitrarily close to the true repeller. In our calculations we keep the distance ϵ from the repeller equal to 0.002 (i.e., for every point obtained by means of PIM there exists at least one point belonging to the true repeller within the distance smaller than ϵ). The plot in Fig. 1(c) obtained with this procedure is consistent with the picture resulting from the previous method; see Fig. 1(b). Again we do not find any characteristic repeller holes that would be transversal to the unstable direction. Comparing the efficiency of both methods we see that the former one gives a better result — there are more points plotted in Fig. 1(b) than in Fig. 1(c), although both pictures are obtained with nearly the same computational time. This is in accordance with the remark of Nusse and Yorke,[17] who state that PIM

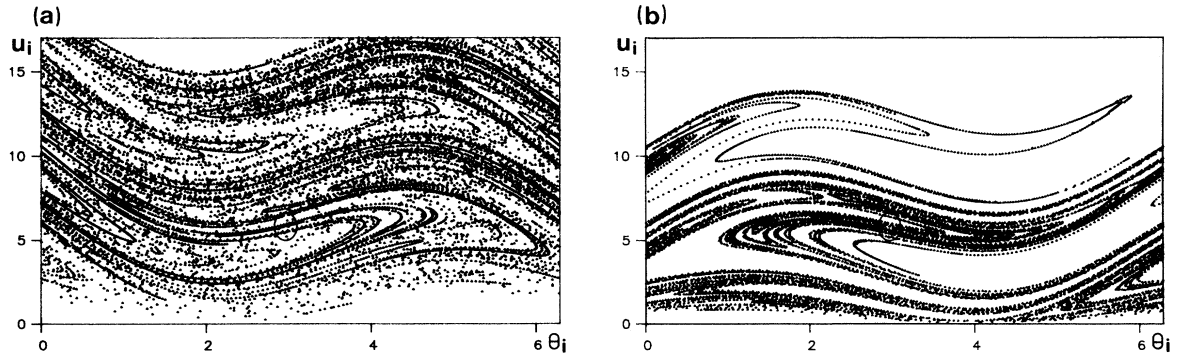

FIG. 3. (a) Stable and (b) unstable manifolds of the unstable fixed point (center of small ellipse). We take a small interval of length 0.02 tangential to the unstable (stable) manifold at point (u^*, θ^*). Next we choose a large number of initial points m_u (m_s) uniformly spread along the interval(s) and each of these points is iterated 14 times forward (backward). Additionally, in the case of the stable manifold we end the backward iterations whenever u_i escapes above 15. Here $m_u = 32\,000$ and $m_s = 44\,000$.

procedure works better for shorter transients, while the former method, introduced by Kantz and Grassberger,[3] is adjusted for longer transients, which is precisely our case.

At the third check we construct the repeller through intersections of the stable and unstable manifolds of an unstable fixed point.[1] Both manifolds are shown in Fig. 3. They are obtained by forward (backward) iterations of the primary (inverse) map. As initial conditions we choose a large number of points spread along unstable (stable) direction in the close vicinity of the one-impact period-1 saddle point $(v^*, \theta^*) = (2\pi, \pi - \phi)$, where $\sin\phi = (1-k)2\pi/\lambda$. The overlap of these two manifolds is shown in Fig. 1(d). The seemingly existing narrow gaps transversal to the unstable direction are not a real effect but a result from a finite number of initial points for the stable manifold calculation. This was checked by plotting a few extra intersections for an increasing number of points. This caused a systematic decrease in the widths of these gaps, which allows us to conclude that the gaps result from a finite statistics. Besides this small difference Fig. 1(d) is fully consistent with Figs. 1(b) and 1(c) obtained with the two other methods.

We notice that the stable manifold in Fig. 3(a) appears to be very "dense" and one can expect its capacity dimension to be close to 2. This can be checked independently by investigating the structure of the basin boundary. The basin boundary is a stable manifold of the saddle point separating the coexisting attractors. Consequently the basin boundary embodies the nontrivial repeller. Our conclusion of the non-double-cantor-type repeller would be consistent with the fact that the stable manifold is a nearly two-dimensional band practically embodying the unstable manifold. For $\lambda = 4.95$ the lowest phase-plane attractor coexisting with the self-reanimating mode is the once-bifurcated Zaslavsky-Rachko[6,16] mode of the two-impact period-6 type. A practical computational problem is that the boundary is so densely tangled that the distinction of borderlines is really an arduous task. In Fig. 4 we have demonstrated this difficulty by blowing up the seemingly solid black basin. By using various refined grids (10 vertical steps)$\times$(10,50,100,1000 horizontal steps) on the same region $[\Delta u, \Delta\theta] = 0.01 \times 0.5$ at around the lower left corner $u = 16.7, \theta \approx 2.56$, more and more striped borderlines emerge out of the black (Fig. 4). To analyze quantitatively the quality of the stable manifold we have calculated the uncertainty exponent α by the method of Grebogi and co-workers.[4,18] First we iterated 500 000 points on a regular grid with $\Delta\theta = 10^{-6}$ on one horizontal line $2.56 < \theta < 3.06$, $u = 16.7$. Despite this amount of points we could not produce more than about 20 000 borderlines out of the black region. Conceivably this small 4% yield may increase the error bars in the calculation. The size of the uncertainty region was calculated as a function of the initial condition inaccuracy $n \times \Delta\theta$ up to four decades ($n = 10^4$) consistently giving the value $\alpha \approx 0.15$ for the slope. This corresponds to the basin boundary box dimension $D_B \approx 2 - 0.15 = 1.85$. The constant emerging of borderlines out of the black (Fig. 4) together with the high boundary dimension indicate that the unstable manifold is nearly embedded in the stable one and their intersections, i.e., the repeller points, must lie on the unstable manifold very densely. This again lends support to the conclusion that the associated repeller has no transversal holes and consequently no double-cantor structure.

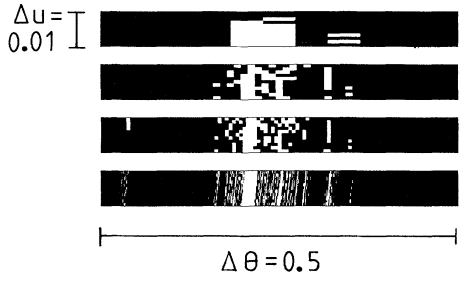

FIG. 4. A stripe of the basin structure at $\lambda = 4.95$, $\theta \in (2.56, 3.06)$, $u \in (16.7, 16.71)$. The black and white denote the basin of the self-reanimating mode and the two-impact period-6 mode [a once-bifurcated Zaslavsky-Rachko mode (Ref. 16)], respectively. To show the structure inside the seemingly solid black basin four refinements of the horizontal grid are made: from the top 10, 50, 100, and 1000 steps, respectively, are included in the calculation. The vertical grid contains 10 steps.

It should be emphasized that the stable manifold touches the unstable one tangentially (Figs. 3 and 5) in a vast region of the phase plane and for wide ranges of the control parameter λ: not only at peculiar isolated values of λ but inside the whole investigated range $4.9 < \lambda < 8.5$. Such a situation is well known for typical nonhyperbolic attractors, but is anomalous for repellers. We conclude that the bouncing-ball model is a paradigm of systems exhibiting repellers with strong nonhyperbolicity. A similar anomaly also arises in the familiar Hénon map for the parameter ranges that are slightly different and possibly less explored than the conventional ones.[19] Consequently the present results should be a warning against a straightforward use of such powerful methods as the thermodynamic formalism and the cycle expansion in chaotic transient studies. Moreover, qualitatively similar pictures showing strong tangencies in invariant chaotic sets were recently detected also in a Hamiltonian system of the chaotic scattering.[20] Therefore it remains an open question what one should call a "typical" chaotic repeller and whether the "anomalous" properties of chaotic transients found here are at all exceptional. For the strange attracting sets a generic example is the Hénon map at its classical parameters rather than the strictly hyperbolic attractors of the baker's map. Maybe the situation for typical repellers is not so complex and maybe most of them are hyperbolic, but certainly one should be aware of the possible difficulties.

It is interesting to notice that the high value of D_B

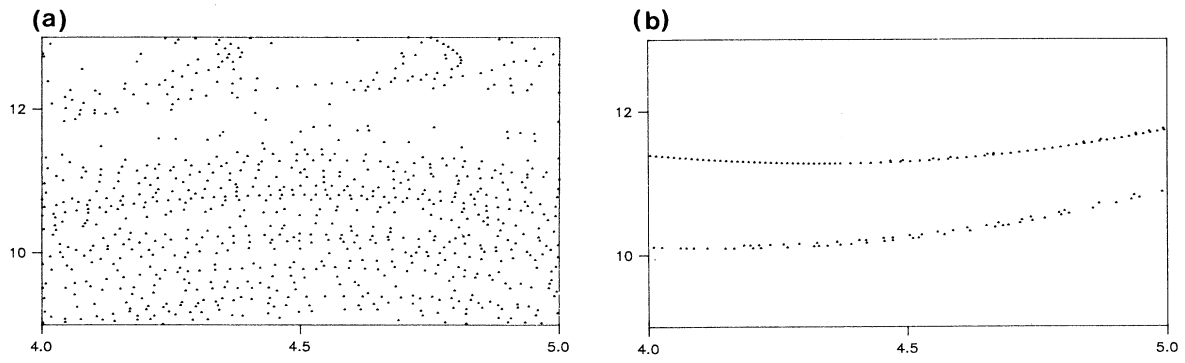

FIG. 5. Enlargement of one of the regions on (u, θ) plane, where the (a) stable and (b) unstable manifolds are tangential.

in a wide range of λ is not the only unexpected feature of the basin boundary in the bouncing-ball dynamics. In Fig. 6 we present a kind of smooth-fractal metamorphosis[18,21] of the black-white boundary between the permanent mute mode ($\tau_i = 0$) and two-impact period-1 mode basins[16] for a representative λ. Moreover, in both structures we have an infinite number of accumulating black bands exhibiting both smooth [Fig. 6(a)] and fractal [Fig. 6(b)] black-white boundaries. No gray-black boundary exists. With increasing control the bands first increase, but finally the fractal fingers of the basin boundary suddenly intrude in the basin diminishing its size drastically. This behavior is important in the technical safety analyses of the stable motions against disturbances. We will return to these questions in a future report.[22] Finally, we note that this geometry (Fig. 6) is very similar, at least up to the first few magnifications, to the truncated fractal and nonfractal structures found recently in the driven pendulum[23] and in the Josephson junction,[24] respectively.

Finally, we want to discuss one anomaly found here in the present study of chaotic transients. At a brief glance the absence of the double-cantor structure of the repeller does not seem to be so exotic. Namely, if even in an ordinary case we would choose the control parameter sufficiently close to and beyond the critical value λ_c of the boundary crisis, the resulting repeller would have an arbitrarily long mean lifetime [Eq. (2)] and the possible transversal holes could be made arbitrarily narrow. Conceivably this would be the case only in the limited neighborhood of the critical control. Moreover, for an ordinary chaotic repeller we would find diminishing lifetimes and wider transversal holes by increasing the control. On the contrary, in the present anomalous dynamics the calculated mean lifetime γ is an increasing function in a wide range of λ as is evident from the plot in Fig. 7. Physically this can be understood as follows. The shapes of the stable and unstable manifolds in the subregion of a small relative velocity u_i, where sticking to surface takes place, do not change significantly with the increase of amplitude λ. Simultaneously the unstable manifold occupies the regions of larger and larger u_i. Consequently a single transient trajectory spends more and more time far from the regions where $\tau_i < \delta$ and where Eqs. (6) and (7) are valid. Therefore we observe an increasing dependence of the mean lifetime γ on the amplitude λ; see Fig. 7.

In conclusion, we have demonstrated that the hyperbolicity, the double-cantor structure, and the

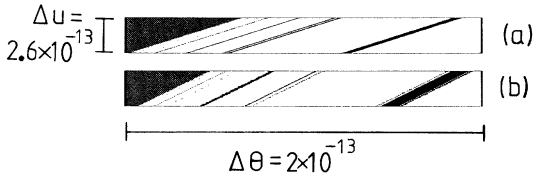

FIG. 6. (u, θ) basins at (a) $\lambda = 2.604$ and (b) $\lambda = 2.79$. The lower left corner coordinates (u, θ) are (a) $\approx (4.768, 5.36)$ and (b) $\approx (4.687, 5.52)$. The white, gray, and black denote the basins of the mute mode, one-impact period-2 Zaslavsky-Rachko mode, and the exotic two-impact period-1 mode, respectively (Refs. 15 and 16). Both black basins exhibit an infinite number of narrow bands accumulating at the gray boundary. Irrespective of the infinite number of the borderlines the black-white boundary is (a) smooth or (b) fractal. No black-gray boundary exists.

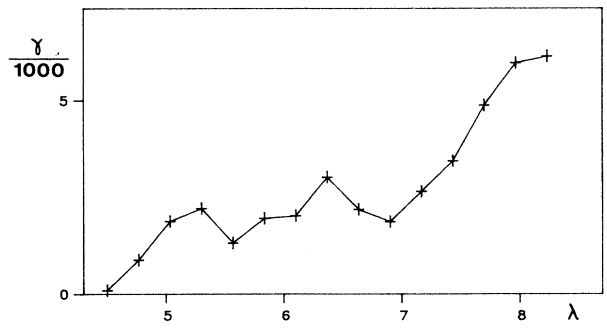

FIG. 7. Mean lifetime γ vs control parameter λ. For each value of λ we have $M_0 = 250$ [see Eq. (1) and Fig. (2)].

monotonously decreasing dependence of the transient mean lifetime on the control beyond the boundary crisis, which are supposed to be characteristic features of ordinary chaotic repellers, need not be generally valid. The present study of a realistic mechanical system, the bouncing-ball model, gives a paradigm of such an anomalous chaotic transient dynamics.

We are grateful to Tamás Tél (Eötvös Loránd University), Michael Thompson (University College London), and James A. Yorke (University of Maryland) for valuable discussions. One of us (M.F.) would like to acknowledge Gert Eilenberger for his warm hospitality during the stay at Institut für Festkörperforschung, Kernforschungsanlage Jülich G.m.b.H. (KFA) and financial support from the Alexander von Humboldt Foundation. We thank the Finnish State Computing Centre Valtion tietokonekeskus (VTKK) and Forschungszentrum KFA for the provision of computational facilities.

---

*On leave from: Higher Educational School, Podchorążych 2 Kraków, Poland.

†The author to whom reprint requests should be directed.

[1]For a recent review see T. Tél, in *Directions in Chaos*, edited by Hao Bai-Lin (World Scientific, Singapore, 1990), Vol. 3, pp. 149–211, and references therein.

[2]C. Grebogi, E. Ott, and J. A. Yorke, Physica D **7**, 181 (1983).

[3]H. Kantz and P. Grassberger, Physica D **17**, 75 (1985).

[4]C. Grebogi, S. W. McDonald, E. Ott, and J. A. Yorke, Phys. Lett. **99A**, 415 (1983); S. W. McDonald, C. Grebogi, E. Ott, and J. A. Yorke, *ibid.* **107A**, 51 (1985).

[5]P. Grassberger, R. Badii, and A. Politi, J. Stat. Phys. **51**, 135 (1988).

[6]G. M. Zaslavsky, Phys. Lett. **69A**, 145 (1978).

[7]P. J. Holmes, J. Sound Vib. **84**, 173 (1982).

[8]R. M. Everson, Physica D **19**, 365 (1986).

[9]M. Franaszek and Z. J. Kowalik, Phys. Rev. A **33**, 3508 (1986).

[10]N. B. Tufillaro, T. M. Mello, Y. M. Choi, and A. M. Albano, J. Phys. (Paris) **47**, 1477 (1986).

[11]T. M. Mello and N. B. Tufillaro, Am. J. Phys. **55**, 316 (1986)

[12]S. Celaschi and R. L. Zimmerman, Phys. Lett. A **120**, 447 (1987).

[13]K. Wiesenfeld and N. B. Tufillaro, Physica D **26**, 321 (1987).

[14]P. Pierański and J. Małecki, Phys. Rev. A **34**, 582 (1986).

[15]Z. J. Kowalik, M. Franaszek, and P. Pierański, Phys. Rev. A **37**, 4016 (1988).

[16]H. M. Isomäki, in *Nonlinear Dynamics in Engineering Systems,* edited by W. Schiehlen (Springer, Berlin, 1990), pp. 125–131.

[17]H. E. Nusse and J. A. Yorke, Physica D **36**, 137 (1989).

[18]C. Grebogi, E. Ott, and J. A. Yorke, Phys. Rev. Lett. **56**, 1011 (1986); Physica D **24**, 243 (1987).

[19]J. A. Yorke (private communication).

[20]Christof Jung (unpublished).

[21]Y. Yamaguchi and K. Tanikawa, Phys. Lett. A **142**, 95 (1989).

[22]H. M. Isomäki and M. Franaszek (unpublished).

[23]M. Varghese and J. S. Thorp, Phys. Rev. Lett. **60**, 665 (1988).

[24]S. Rajasekar and M. Lakshmanan, Phys. Lett. A **147**, 264 (1990).